Bioconjugate Chemistry

Article

pubs.acs.org/bc

Long-Term/Bioinert Labeling of Rat Mesenchymal Stem Cells with PVA-Gd Conjugates and MRI Monitoring of the Labeled Cell Survival after Intramuscular Transplantation

Yoichi Tachibana,[†] Jun-ichiro Enmi,[‡] Carlos A. Agudelo,[†] Hidehiro Iida,[‡] and Tetsuji Yamaoka*[,†]

[†]Department of Biomedical Engineering and [‡]Department of Investigative Radiology, National Cerebral and Cardiovascular Center Research Institute, Suita, Osaka 565-8565, Japan

Supporting Information

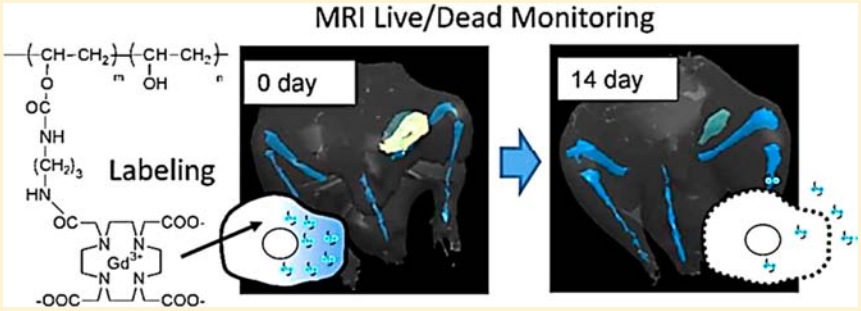

ABSTRACT: Noninvasive in vivo imaging of transplanted stem cells is an effective method to clarify the mechanisms involved in stem cell transplantation therapy. We labeled rat mesenchymal stem cells (MSCs) with water-soluble magnetic resonance imaging (MRI) contrast agent poly(vinyl alcohol)-gadolinium (PVA-Gd) in order to ascertain the fate of transplanted MSCs in vivo. PVA-Gd was retained and localized in the cytosolic compartment of MSCs for a longer period of time. The effect of PVA-Gd labeling on MSC proliferation was much less than that of the commercially available contrast agent ProHance, and the labeled MSCs were found to have osteoblastic differentiation ability. To study the MSC lifetime in vivo, MSCs were seeded and trapped in the cytocompatible three-dimensional porous scaffolds of Spongel and transplanted. The MRI signal attributed to MSCs was eliminated from the transplanted site in 14 days. Because free PVA-Gd was rapidly eliminated from the site, this signal reduction indicated MSC death in the transplantation site. The low efficiency of MSC transplantation for ischemic tissue may be due to their short lifetime, making it important to develop highly effective stem cell transplantation systems that address cell number, injection position, and cell formulation (suspension, sheet, and aggregates). Our cell survival tracking system would be a very powerful tool to this end and would be applicable in clinical cell therapies.

INTRODUCTION

There is an increasing interest in stem cell transplantation therapy because certain types of stem cells can be easily obtained from patients, eliminating the controversy over the use of embryonic stem cells.[1] In particular, autologous mesenchymal stem cells (MSCs) have received much attention because they can differentiate into numerous cell types without being rejected immunologically.[2] Various diseases such as limb ischemia,[3] infarcted myocardium,[4] and brain injury[5] have been treated by MSC transplantation. Recently, Lipinski et al. reported a clinical improvement of 3%, compared to that of the control, in the left ventricular ejection fraction after MSC transplantation.[6] Although the detailed mechanisms of MSC actions in vivo remain unclear, recent studies have focused on paracrine mechanisms. For example, Ziegelhoeffer et al. reported that transplanted MSCs did not promote neovascularization through incorporation into the vessel walls.[7] It is also reported that the transplanted allogenic MSCs decrease within 3 weeks after injection according to the histological analysis.[8] Counting the number of cells in the tissue sections is a good direct method of measuring; however, it is quite difficult to fully understand the behavior of the transplanted cells. The cells might have dispersed and died.

To clarify the behavior of transplanted MSCs globally and quantitatively, in vivo imaging modalities are useful. Among the imaging modalities, magnetic resonance imaging (MRI) is a promising system for cell tracking because of its high resolution and noninvasiveness.[9] There are two important factors to consider in the long term tracking of transplanted cells using MRI: the retention of the contrast agent in the transplanted cells and the elimination of the contrast agent when it leaks from the cells upon cell death. In the last 10 years, the use of superparamagnetic iron oxide (SPIO) particles to label cells has emerged because of its high sensitivity.[10−13] However, some disadvantages of using SPIO particles in this tracking system have been reported.[14−20] The SPIO molecule may be

Received: February 16, 2014
Revised: June 8, 2014
Published: June 13, 2014

exocytized from the cells as time passes. In addition, when the cells die, the SPIO particles go out of the cells. These free particles would remain at the site for a long period of time and may be taken up by the macrophages.

We reported the water-soluble gadolinium (Gd)-based MRI contrast agent for cell labeling and tracking for the first time.[21] Gd-chelate molecules were conjugated to the side hydroxyl groups of poly(vinyl alcohol) (PVA), which interacts with macrophages or blood cells very weakly due to its high hydrophilicity.[22] The novel polymeric MRI contrast agent, PVA-Gd, was quickly eliminated when injected intramuscularly, which is the biggest advantage of our system in comparison with the system using SPIO. We delivered PVA-Gd into model NIH-3T3 cells by electroporation and proved that more than 90% of PVA-Gd remained localized in the cytosolic compartment at 10 days after labeling. The concentration of Gd in a single cell decreased upon cell division, but the total signal intensity of living cells did not change and remained at the site of injection. In addition, using a similar water-soluble MRI imaging agent[23,24] we observed that CD34-positive cells in the peripheral blood spread and migrate from the site of injection, which also leads to the decrease in the MRI contrast.

We have been working on the transplantation of various kinds of stem cells to the rat hindlimb ischemia models. Despite numerous reports on the MSC transplantation to ischemic tissues,[25,26] the blood flow recovery does not always appear to be satisfactory.[27] Even by the evaluation of an infrared laser-Doppler blood flow meter (see Supporting Information 1) satisfactory blood flow recovery could not be achieved. Thus, the fate of the transplanted cells arose as one of the biggest research targets. In the present study, we verified the fate of the transplanted MSCs labeled with the PVA-Gd in vivo using MRI for long periods of time. Furthermore, unlike the model NIH-3T3 cells,[22] the maintenance of MSC potential is very important. We then evaluated the efficacy and safety of PVA-Gd by testing the differentiation potential of the PVA-Gd labeled MSCs, determining their intracellular distribution, and quantifying the duration of the cellular retention of PVA-Gd in vitro. Because not only the mechanism of angiogenesis, but also MSC differentiation into endothelial or smooth muscle cells, has been under debate,[25,26] we evaluated the well-established differentiation of MSCs into osteoblasts using PVA-Gd labeling. In addition, to differentiate cell disappearance (death) from cell diffusion or migration, the three-dimensional porous scaffolds, Spongel, was used to retain the seeded MSCs in the 3D structure, and the disappearance of the labeled MSCs was monitored in vivo using MRI for 2 weeks.

RESULTS AND DISCUSSION

Labeling of rMSCs. Electroporation is a convenient means to introduce various substrates into different kinds of cells.[28,29] By this method, substrates are introduced nonspecifically and directly in cells, and not via the endocytosis pathway. However, cells might be damaged by electroporation depending on conditions such as voltage or irradiation time. We established and used a mild condition to deliver F-PVA-Gd into cells. To confirm the delivery of F-PVA-Gd into rMSCs, the cells were observed under a fluorescence microscope immediately after electroporation (Figure 1a) and all rMSCs were found to be labeled with F-PVA-Gd. Interestingly, F-PVA-Gd was localized in the cytosolic compartments and not in the nucleus indicating the direct introduction of F-PVA-Gd into rMSCs. After 10 days of cell proliferation, the F-PVA-Gd staining in rMSCs was similar to the staining at day 0, indicating that PVA-Gd was evenly distributed in the two daughter cells during mitosis and that it remained in the cytosolic compartment (Figure 1b).

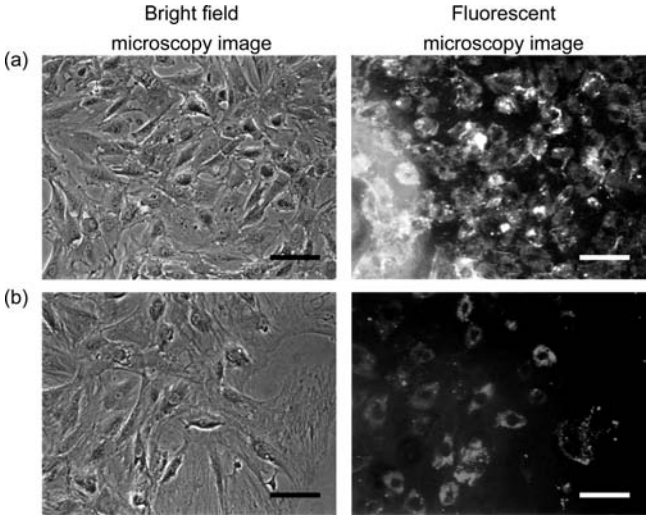

Figure 1. Phase contrast and fluorescent images of rat MSCs (a) 0 and (b) 10 days after labeling with F-PVA-Gd. The bright rings in the fluorescent images matched to the cytosolic compartments. The scale bar represents 20 μm.

Proliferation of F-PVA-Gd- and ProHance-Labeled rMSCs. Proliferation of F-PVA-Gd- and ProHance-labeled rMSCs was determined by counting the cells with a hemocytometer (Figure 2). ProHance was selected as a control because it is widely used in clinical settings.[30] In both cases, the number of rMSCs increased over time. However, the proliferation rate of F-PVA-Gd-labeled rMSCs was about 1.3 times higher than that of ProHance-labeled rMSCs. Although acute cytotoxicity was not observed immediately after cell labeling (data not shown), the proliferation rate of rMSC was slightly affected by ProHance labeling. A previous study clearly indicated that the long-term effect of contrast agents on cells in vitro and in vivo must be assessed in detail for the development of a successful cell tracking system.[31] Brekke et al. reported no detrimental effects of the contrast agent on neural stem cell viability, migratory capacity, and multipotency. Nevertheless,

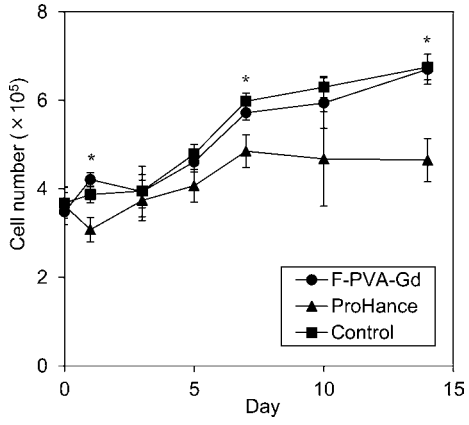

Figure 2. Growth of rat MSCs labeled with (●) F-PVA-Gd and (▲) ProHance. Nonlabeled rat MSCs were used as a control. The data were derived from 3 independent experiments, *$p < 0.05$ compared to ProHance.

the proliferative capacity of the cells was reduced, and the in vivo functional capacity of the cells was largely annihilated.[32] Furthermore, the proliferation of nonlabeled rMSCs was similar to that of F-PVA-Gd-labeled rMSCs (Figure 2).

In our study, proliferation of F-PVA-Gd-labeled rMSCs was faster than that of ProHance-labeled rMSCs. It is known that Gd ions tightly bind DOTA and form stable chelates.[33] However, free Gd ions released from stable chelates may still affect cell proliferation. For clinical use, DOTA-calcium chelates, which are the capture agents for free Gd ions, were added to DOTA-Gd to reduce toxicity. The Gd/DOTA ratio of F-PVA-Gd was 0.54, and the remaining DOTA (0.46) was vacant (i.e., not bound to Gd). Therefore, when Gd was released from the chelates, it was likely that F-PVA-Gd recaptured the free Gd ions more readily than ProHance because the capture agents (empty DOTA) were in the same vicinity as the free Gd ions.

Intracellular Retention of F-PVA-Gd and ProHance. The intracellular retentivity of F-PVA-Gd and ProHance in rMSCs was assessed by measuring the total amount of Gd in the proliferating rMSCs over time using ICP-MS (Figure 3).

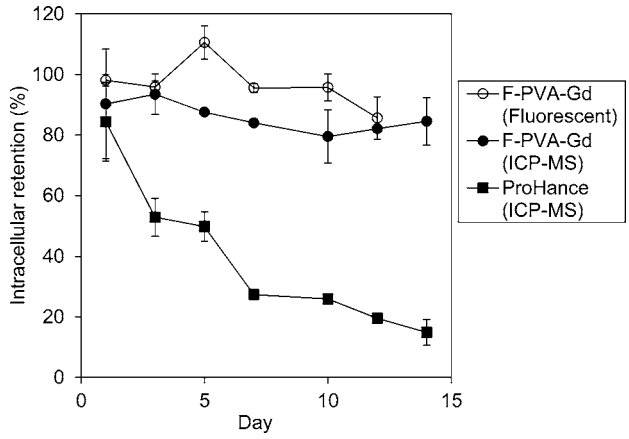

Figure 3. Intracellular retentivity of (● and ○) F-PVA-Gd and (■) ProHance transferred into rat MSCs by the electroporation. The amounts of substances were measured by ICP-MS (● and ■) or the fluorescent intensity of FITC bound to PVA backbone (○). Intracellular retentivity was defined as $A_t/A_0 \times 100$, where A_t and A_0 were the amount of Gd in the rat MSCs at days t and 0, respectively. The data were derived from 3 independent experiments.

Labeled rMSCs were cultured for a given period of time without subculture and were then lysed. Before lysing rMSCs, they were sufficiently washed with PBS to eliminate any attached F-PVA-Gd and ProHance from the cells. The total amount of F-PVA-Gd in rMSCs did not change significantly even after 14 days. In contrast, the total amount of ProHance in rMSCs decreased gradually, and only 10% of ProHance remained in rMSCs on day 14. To confirm the intracellular retentivity of F-PVA-Gd, fluorescence measurements of the cell lysate were performed (Figure 3, open circles). Fluorescence derived from F-PVA-Gd in rMSCs showed no change over 12 days. Similar results for Gd concentration and fluorescence indicate that the PVA backbone and Gd molecules are conjugated substantially even inside the cells explaining why F-PVA-Gd remains in the cytosolic compartment for a long period, as observed in Figure 1.

After labeling, low molecular weight Gd-chelates like ProHance readily exit out of cells, as shown in Figure 3. This decrease in the cellular Gd results in the loss of MRI signal after cell transplantation, and does not allow the understanding of cell behavior, including cell movement, proliferation, and death. Endres et al. synthesized Gd-DOTA-SS-Arg_8 to prolong the retention time of Gd in cells.[34] Twenty-four hours after transfection, Gd-DOTA-SS-Arg_8 remained in 40% of the cells. However, contrast agents must remain in cells in a retentive condition for at least 2 weeks in order to conduct successful long-term cell tracking in vivo using MRI. The excellent intracellular retention is one of the most important features of our system. Because the labeling of stem cells using conventional SPIO is based on the endocytosis, the internalized SPIO cannot be retained in the cells for a longer period of time.

Differentiation of F-PVA-Gd-Labeled rMSCs. To evaluate the multipotency of rMSCs after labeling, F-PVA-Gd-labeled rMSCs were treated with an osteogenic medium for 3 weeks (Figure 4). Osteogenic differentiation was evaluated using morphological and biochemical techniques. After confirming the introduction of F-PVA-Gd into rMSCs, they were plated and treated with the differentiation medium. Nodular aggregates of cells were observed on day 7, and they increased until day 21 (Figure 4a). Furthermore, the aggregates became larger over time. The mineralization capability of rMSCs was also evaluated (Figure 4b). The nodular aggregates were stained with alizarin red S, which is a widely used indicator of mineralization. Alizarin red-positive nodular aggregates were present on day 11. On day 21, alizarin red-positive aggregates became larger and showed more intense staining, indicating more extensive mineralization. These results clearly show that the differentiation ability of rMSCs is not affected by F-PVA-Gd. For effective stem cell therapies, labeling agents must not inhibit the ability of cells to differentiate. Our results suggest that F-PVA-Gd-labeled MSCs can differentiate into functional cells in vivo, and that the transplanted cells can be detected by MRI. The maintenance of the plasticity of the stem cells is very important. The differentiation of SPIO-labeled MSCs either in vitro or in vivo has been reported,[14] and a recent study showed that ferumoxide (dextran-coated SPIO) labeling did not alter the function or differentiation capacity of MSCs.[15] In contrast, Farrell et al. suggested that SPIO labeling of MSCs may alter the expression of the osteogenic marker CBFA1.[16]

In Vitro MRI of F-PVA-Gd-Labeled rMSCs. To perform an MRI of rMSCs, labeled rMSCs were uniformly fixed in agarose gels. Figure 5 shows the T_1-weighted images of different densities of cells labeled with F-PVA-Gd in 2% agarose gel. The measurement of all the samples was performed simultaneously. The signal was enhanced in the gel containing more than 7.5×10^6 labeled cells. Furthermore, T_1 values of the samples with 0, 4.9×10^6, 7.5×10^6, and 1.4×10^7 cells were estimated with least-squares fitting of the signal intensities measured at nine TR values in an exponential fashion (see Supporting Information 2). As expected, the T_1 value reduced with an increased the number of cells (1029 ms at 0; 519 ms at 4.9×10^6; 454 ms at 7.5×10^6; and 265 ms at 1.4×10^7). Longitudinal relaxation rate (R_1) was linearly correlated with the number of labeled cells (see Supporting Information 2). The signal of 4.9×10^6 cells was slightly higher than that of control agarose gel, suggesting that the F-PVA-Gd-labeled cells are detectable due to the enhanced signal intensity of the surrounding water around the PVA-Gd molecules in the cell. However, the signal intensity may change with the environment around PVA-Gd. Therefore, the relationship between MR

dx.doi.org/10.1021/bc400463t | Bioconjugate Chem. 2014, 25, 1243−1251

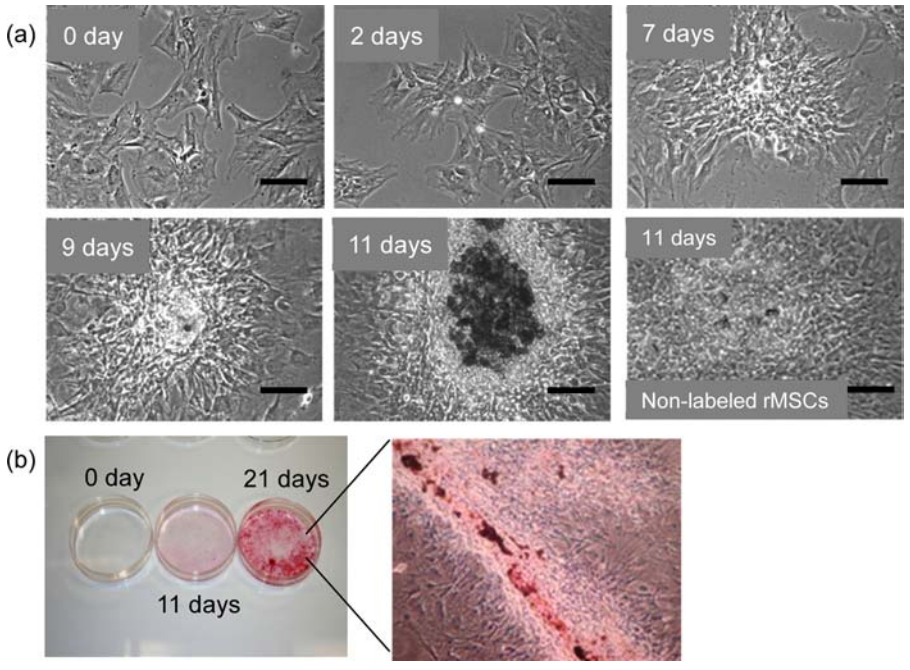

Figure 4. (a) Photographs of rat MSCs labeled with F-PVA-Gd and nonlabeled rat MSCs cultured in osteogenic induction medium (DMEM supplemented with 10 nM dexamethasone, 10 mM β-glycerophosphate, and 50 μM ascorbic acid). The scale bar represents 20 μm. (b) Alizarin red S staining of the MSCs at 0, 11, and 21 days.

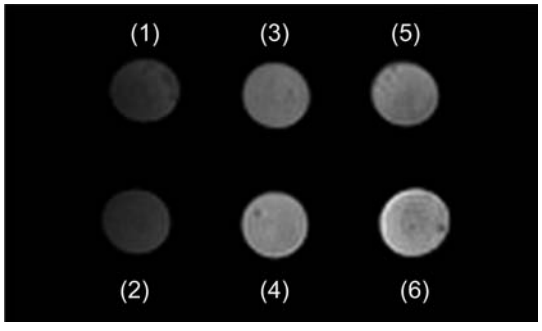

Figure 5. MR images of F-PVA-Gd-labeled MSCs embedded in 2 wt % agarose gel at the cell concentration of (1) 0, (2) 1.0×10^6, (3) 5.0×10^6, (4) 7.5×10^6, (5) 1.0×10^7, and (6) 2.0×10^7 cells/100 μL. T_1-weighted images of the samples were acquired at TE of 9 ms and TR of 1000 ms using a 3D spin echo sequence (FOV, 4 × 8 cm; matrix, 128 × 256; slice thickness, 1 mm; slice gap, 0 mm; number of slices, 35).

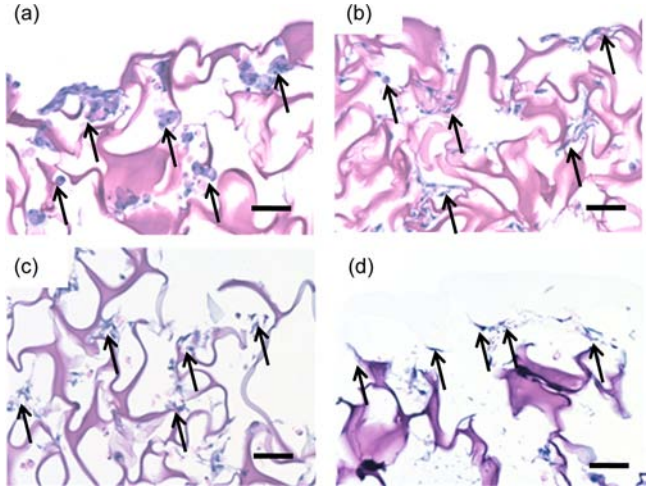

Figure 6. HE staining of labeled rat MSCs seeded into Spongel and cultured for (a) 1, (b) 3, (c) 7, and (d) 14 days in DMEM medium. The arrowhead indicates the adherent cells. The scale bar represents 50 μm.

signal and the state of water around PVA-Gd in the intracellular crowding conditions needs to be addressed in future studies.

In Vivo MRI Tracking of F-PVA-Gd-Labeled rMSCs. To track F-PVA-Gd-labeled rMSCs without affecting cell migration in vivo, labeled rMSCs were seeded on a gelatin sponge in vitro. HE staining was performed on culture days 1, 3, 7, and 14 (Figure 6). A day after seeding, the labeled rMSCs adhered to the surface of the gelatin sponge. The gelatin sponge was swollen to about twice its original size in the culture medium on day 14, and the adhesion of rMSCs was still observed. This confirmed that rMSCs adhered to the sponge and distributed homogeneously not only on the surface but also in the middle area of the sponge.

For in vivo imaging, labeled rMSCs (1.3×10^7 cells) were seeded on the gelatin sponge as described above. After 1 day in culture, the labeled rMSCs/sponge construct was implanted into the femoral muscle of ischemic rats. Even 7 days after transplantation, it was possible to identify the transplanted rMSCs in vivo at the original site of implantation by MRI (Figure 7); however, there was no sign of cell migration. In contrast, on day 14, contrast enhancement attributed to rMSCs could not be observed on the sponge. We constructed a 3D model from a series of two-dimensional slices, as shown in Figure 8. We clearly observed that the signals of the transplanted rMSCs (yellow color) were slightly reduced on day 14, while the signals of the sponge (aqua blue color) still remained at the area where the labeled rMSCs were originally transplanted. Similar results were obtained in all seven rats (see Supporting Information 3a). On day 28, the sponge could not be detected due to degradation (data not shown). These results strongly suggested that MSCs implanted into the ischemic

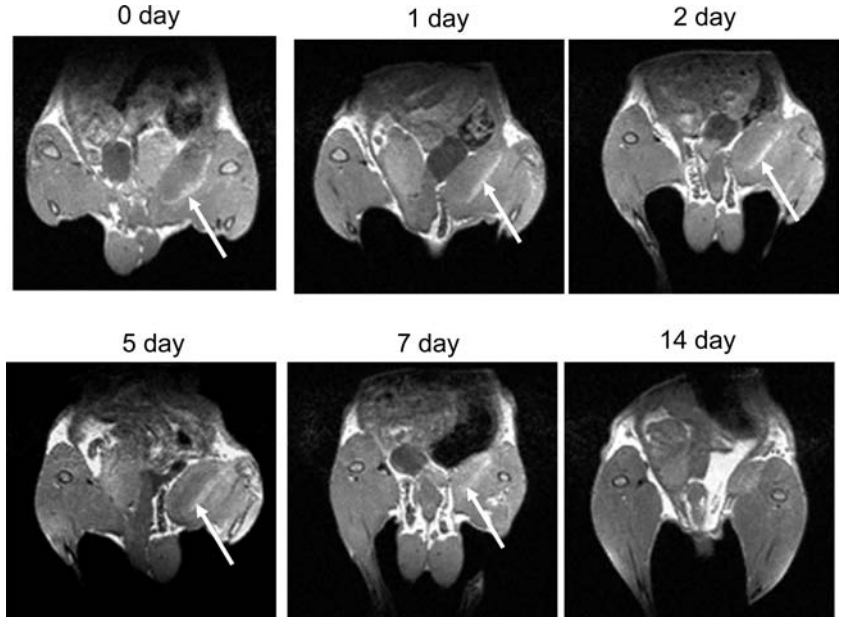

Figure 7. In vivo T_1-weighted 1.5 T MR images of rats transplanted with rMSCs/Spongel constructs at TR of 1500 ms and TE of 9 ms (FOV, 4 × 8 cm; matrix, 128 × 256; slice thickness, 1 mm; slice gap, 0 mm; number of slices, 35). White arrows indicate the contrast resulting from the cells.

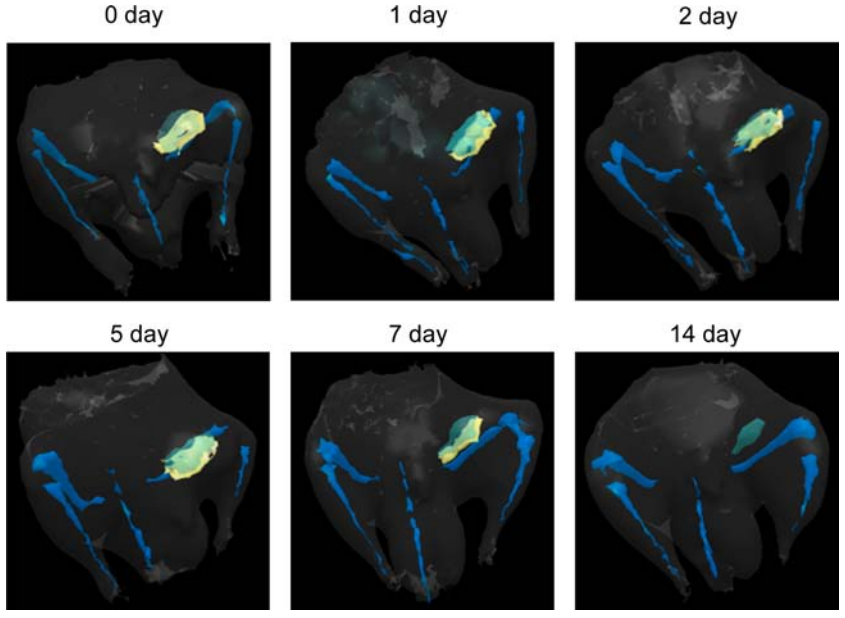

Figure 8. Three dimensional images of transplanted MSCs/Spongel constructs. Yellow color indicates the transplanted cells, aqua blue color indicates the Spongel, and blue color indicates the bone.

region through porous scaffolds do not migrate outside the sponge, but are eliminated by another mechanism. The nonlabeled rMSCs/sponge constructs or original sponge did not give us any positive MRI signal (Supporting Information 3b).

The cell environments in vitro and in vivo are very different. Proliferation may be more active in the culture medium than in vivo, because the culture medium is optimized for cell proliferation. It is assumed that lower division rates of the transplanted cells can lead to higher intracellular retention of PVA-Gd in vivo and possibly higher contrast in vivo compared to the contrast obtained in vitro.

In the past, several groups have demonstrated MSC tracking in vivo. Farrell et al. reported that MSCs transplanted subcutaneously could be tracked in vivo for 4 weeks after transplantation.[16] Furthermore, SPIO-labeled MSCs transplanted into the infarcted heart of rats could be tracked for at least 16 weeks.[11] However, cell distribution was not quantified in vivo. Our results demonstrated that a majority of the transplanted rMSCs could not be observed 14 days after transplantation (Figures 7 and 8). We confirmed that the proliferation of labeled rMSCs on day 14 was approximately twice as much as that on day 1 in the culture (Figure 2), and F-PVA-Gd was still retained in rMSCs (Figure 3). The amount of F-PVA-Gd in rMSCs became half of its original amount on day 14 after transplantation, and this amount was sufficient for detection by MRI. Even in cases where the transplanted rMSCs

Scheme 1. Synthesis of PVA-Gd MRI Contrast Agent for Stem Cell Labeling

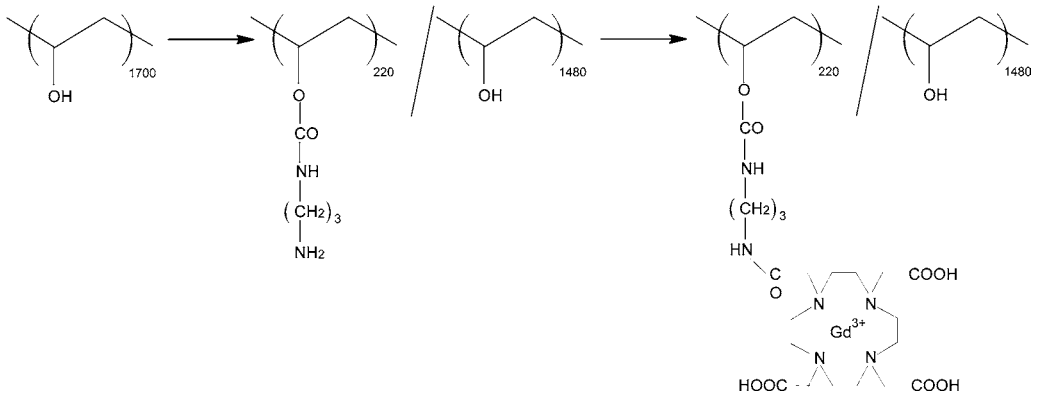

are differentiated into other lineages, the transplanted cells could be detected due to the internalization of F-PVA-Gd.

In the case of SPIO, the contrast may remain at the site even after SPIO somehow exits the cells. Some studies have shown that free SPIO may either be internalized by macrophages or remain at the site of cell transplantation.[17−20] This leads to unexpected MRI contrast results regardless of the in vivo localization of the transplanted stem cells. There are two possible reasons for the disappearance of MSC signal at the site of implantation in the present study. One reason is that the transplanted rMSCs diffuse, but we confirmed the effective retention and survival of MSCs in Spongel, which should be same even in vivo. The other reason is cell death within 14 days. According to the MRI images in Figure 8, the area size of the detected cells (yellow area) did not enlarge over time and the signal intensity gradually decreased. These data suggest that the transplanted cells died rather than diffusing out in the body. It was reported that MSC transplantation attenuated left ventricular remodeling 2 months after transplantation.[35] Although the curative role of the transplanted rMSCs is unclear in the present study, the transplanted rMSCs disappeared before a complete cure was achieved. Therefore, the transplanted rMSCs may promote neovascularization in the ischemic area by a paracrine mechanism.

An important feature of cell tracking agents is the low organ/tissue accumulation in their free form. In our previous study,[24] Gd clearance from the rat body was investigated. After dosing Dextran-Gd to the rat, the cumulative dose percentages of Gd were approximately 0.00074% in the kidneys and 0.00089% in the liver. These values were extremely low in comparison with the total dosage, demonstrating the biocompatibility. We previously reported that the organ/tissue accumulation of PVA is much less than dextran and quite similar to those of poly(ethylene glycol) (PEG), whose bioinertness is well-known. PVA with many hydroxyl groups is different from PEG and is a desirable base polymer.

CONCLUSION

We described a novel PVA-based contrast agent for MRI (F-PVA-Gd) to label MSCs, which could be translated for use in clinical cell therapy. Proliferation of F-PVA-Gd-labeled rMSCs was faster than that of ProHance-labeled rMSCs. Differentiation of labeled rMSCs was not affected by F-PVA-Gd, which may be the result of the high retentivity and hydrophilicity of F-PVA-Gd. In addition, F-PVA-Gd was retained in the cytosolic compartment of rMSCs for at least 14 days. Furthermore, in vivo T_1-weighted images of rMSCs revealed that rMSCs are eliminated with time from the site of transplantation within 14 days even when the stem cells are seeded and trapped in the porous gelatin scaffold, Spongel. In conclusion, we can now noninvasively visualize cellular behavior in vivo, and our cell tracking system will be a powerful tool for studying the lifespan of transplanted cells and developing the most effective transplantation methods for stem cell therapy.

MATERIALS AND METHODS

Materials. PVA (MW, 74,800; degree of saponification, 98%) was a kind gift from Kuraray Co. Ltd. (Okayama, Japan). 1,4,7,10-Tetraazacyclododecane-1,4,7,10-tetraacetic acid mono-(*N*-hydroxysuccinimidyl ester) (DOTA-NHS-ester) was purchased from Macrocyclics (Dallas, TX). Fluorescein isothiocyanate (FITC)-NHS-ester was purchased from Invitrogen (Eugene, OR). Gd chloride ($GdCl_3$) was purchased from Wako Pure Chemical Industries (Osaka, Japan). Resovist was purchased from Nihon Schering (Osaka, Japan). Other reagents and solvents were commercially available and used as received.

Synthesis of Fluorescein-Labeled PVA-Gd (F-PVA-Gd). PVA-Gd was synthesized according to our previous report.[21] In brief, a mixture of PVA (0.44 g, 10 mmol in monomer unit concentration) and carbonyl diimidazole (7.5 mmol) was stirred in 80 mL of anhydrous dimethyl sulfoxide (DMSO) at room temperature for 4 h under a nitrogen-rich atmosphere. Next, 1,3-propanediamine (7.5 mmol) was added to the mixture, and the mixture was further stirred at room temperature for 1 day, and dialyzed using the Spectra/Por membrane (cutoff molecular weight = 1×10^4; Spectrum Laboratories, Inc., Rancho Dominguez, CA) against distilled water three times, and finally lyophilized to yield aminated PVA. The aminated PVA was then dissolved in 80 mL of anhydrous DMSO and reacted with DOTA-NHS-ester and FITC-NHS-ester at room temperature for 1 day under a nitrogen-rich atmosphere. The reaction mixture was dialyzed against distilled water three times and lyophilized to give fluorescein-labeled chelated PVA. The solution of fluorescein-labeled chelated PVA was then treated by the dropwise addition of 1.5 mol equiv of $GdCl_3$ to DOTA while stirring. The pH was maintained between 6.6 and 7.0 with 1 M NaOH solution and stirred at room temperature for an additional 24 h. The reaction mixture was dialyzed against distilled water three times and lyophilized to produce F-PVA-Gd (Scheme 1).

^{1}H NMR spectra were recorded on a 300 MHz NMR spectrometer (Gemini2000/300; Varian Inc., CA) with a sample concentration of 8 mg/800 μL. The concentration of

dx.doi.org/10.1021/bc400463t | *Bioconjugate Chem.* 2014, 25, 1243−1251

the paramagnetic species [Gd(III)] was measured by inductively coupled plasma atomic emission spectroscopy (ICP-AES) (Model 7510, Shimadzu Co., Kyoto, Japan).The introduction ratio of DOTA per PVA unit was 12.9 mol % by using ^{1}H NMR and the Gd content was 11.5 wt %, and a reflexivity value of F-PVA-Gd was 7.0 mM^{-1} s^{-1}

Rat MSCs (rMSCs). rMSCs were isolated from rat marrow aspirates. The aspirates were washed with PBS three times and cultured in low glucose Dulbecco's modified Eagle's medium (DMEM) supplemented with 10% bovine calf serum, 5% horse serum, 100 units/mL penicillin, and 100 units/mL streptomycin at 37 °C under 10% CO_2 atmosphere. All experiments were performed using fourth-passage rMSCs.

F-PVA-Gd Labeling of rMSCs by Electroporation. First, rMSCs were cultured in a 6 cm Petri dish at a concentration of 5×10^5 cells/dish in culture medium for 1 day. Cells were washed with PBS three times, and fresh culture medium without serum was added. Next, F-PVA-Gd or ProHance [gadolinium 1,4,7-tris (carboxymethyl)-10-(2′-hydroxypropyl)-1,4,7,10-tetraazacyclododecane] at a final Gd concentration of 10 mM was added to the culture medium. Electrical pulses were applied to cells using a CUY-21 electroporator (NEPPA GENE, Tokyo, Japan). Rectangular electrical pulses (field strength, 300 V/cm; number of pulses, 10; pulse duration, 5 ms) were applied to cells using two parallel electrodes with a 5 mm gap. After applying electrical pulses, cells were incubated for 1 h and washed twice with PBS.

Intracellular Retentivity of F-PVA-Gd in rMSCs. The intracellular retention of F-PVA-Gd was evaluated using two approaches. The first approach was to directly measure the amount of Gd in cells using an inductively coupled plasma mass spectrometer (ICP-MS; ICPM-8500, Simadzu, Kyoto, Japan). The second approach was to measure the fluorescence intensity of the PVA molecules coupled to FITC. F-PVA-Gd- or ProHance-labeled rMSCs were harvested with 0.025% trypsin, washed with PBS, suspended in 1 mL nitric acid, heated at 90 °C for 6 h, and diluted in water. The amount of Gd in the cell lysates was measured using ICP-MS. The intracellular retentivity was calculated as $A/A_0 \times 100$, where A and A_0 represent the total amount of Gd in rMSCs at a given day and immediately after electroporation, respectively. The harvested cells were suspended in 1 mL cell lysis buffer [25 mM Tris (pH = 7.8), 2 mM dithiothreitol, 2 mM 1,2-diaminocyclohexan-*N*,*N*,*N*′,*N*′-tetraacetic acid, 10% glycerol, 1% Triton X-100] and incubated for 1 h at 37 °C. The fluorescence intensity was measured using a spectrofluorometer (Wallac 1420 ARVOsx; PerkinElmer Life Sciences, Boston, MA; excitation, 430 nm; emission, 540 nm). The intracellular retentivity was calculated as $F/F_0 \times 100$, where F and F_0 represent the total fluorescence intensity of the cell lysate at a given day and immediately after electroporation, respectively.

Osteogenic Differentiation of F-PVA-Gd-Labeled rMSCs. F-PVA-Gd-labeled rMSCs were cultured in a 6 cm Petri dish at a concentration of 5×10^5 cells/dish for 1 day, and the medium was changed with induction medium, DMEM supplemented with 10 nM dexamethasone, 10 mM β-glycerophosphate, and 50 μM ascorbic acid. Microscopic observations were performed on days 0, 2, 7, 9, and 11. For alizarin red S staining, cells were washed three times with PBS and fixed with methanol (−2 °C, 2 min), rinsed three times with water, and stained with alizarin red S (5 mg/mL in PBS) for 8 min. After staining, cells were rinsed six times with water.

MRI of rMSCs in Vitro and in Vivo. MRI of rMSCs in vitro was performed as follows. After electroporation, cells were trypsinized in 0.025% trypsin diluted in PBS and washed with PBS. Suspensions with different rMSC densities (0, 1×10^6, 5×10^6, 7.5×10^6, 1×10^7, and 2×10^7 cells/100 μL of 2 wt % agarose solution) were cooled to form gels. MRI data of these gels were collected using a 1.5 T compact MRI system with a permanent magnet (MRmini, Dainippon Sumitomo Pharma, Osaka, Japan) at TE, 9 ms; TR, 1000 ms; FOV, 4×8 cm^2; matrix, 128×256; slice thickness, 1 mm; slice gap, 0 mm; and number of slices, 35). The experimental protocols were approved by the Animal Care Committee of the National Cerebral and Cardiovascular Center Research Institute

MRI of Labeled rMSCs/Porous Sponge Construct in Vivo. In order to prevent the migration of the transplanted cells in vivo, a medical grade porous sponge (Spongel, Astellas, Tokyo, Japan) was used as the scaffold for rMSCs. A labeled rMSC suspension at a density of 1×10^6 cells/100 μL was poured on the porous gelatin scaffold and incubated at 37 °C for 2 h. Fresh medium (400 μL) was added to the gelatin scaffold, and the cells were cultured for 1, 3, 7, and 14 days. After culturing, frozen sections of the gelatin scaffold were prepared using Tissue-Tek (Sakura Finetechnical Co. Ltd., Tokyo, Japan) and stained with hematoxylin and eosin (HE).

Unilateral hind limb ischemia was induced in 8-week-old male F344 rats by ligating and resecting the left femoral artery, vein, and their branches under isoflurane anesthesia (1.5% in air). Rats were then transplanted with the labeled rMSCs/sponge construct, and MRI measurements were performed at 0, 1, 2, 5, 7, and 14 days using a 1.5 T-MR scanner. Rats (n = 8) were again anesthetized with isoflorane and imaged in the dorsal position. Images were acquired in a coronal plane using the spin echo sequence (TE, 9 ms; TR, 1000 ms; FOV, 4×8 cm^2; matrix, 128×256; slice thickness, 1 mm; slice gap, 0 mm; number of slices, 35). The segmented image stacks were used to generate a three-dimensional (3D) model of the transplanted cells, gelatin sponge, and abdominal body of the rats using 3D-Doctor (v 4.0 Able Software Corp, Lexington, MA). The region of the transplanted cells was estimated with careful consideration of the position and size of implanted Spongel, which was seen as slightly dark area, and found a bright signal in the estimated region.

Ethics Statements. All animal experiments were conducted in accordance with the Guidelines for Animal Experiments established by the Ministry of Health, Labor, and Welfare of Japan, and by the National Cerebral and Cardiovascular Center Research Institute, Japan. The protocol was approved by the Committee on the Ethics of Animal Experiments of the National Cerebral and Cardiovascular Center Research Institute (Permit Number: 10047).

■ ASSOCIATED CONTENT

Ⓢ Supporting Information

Blood flow ratio, relaxation times, and MR images as described in text. This material is available free of charge via the Internet at http://pubs.acs.org.

■ AUTHOR INFORMATION

Corresponding Author

*Tel: +81-6-6833-5012 ext 2637. Fax: +81-6-6835-5476. E-mail: yamtet@ri.ncvc.go.jp.

Notes

The authors declare no competing financial interest.

■ ACKNOWLEDGMENTS

This work was supported by grants-in-aid from the Ministry of Health, Labor, and Welfare of Japan (Health and Labor Sciences Research Grants, research on Nanotechnical Medical). This work was also supported by a Research Grant for Cardiovascular Diseases (18A-2) from the Ministry of Health, Labor, and Welfare of Japan. The authors thank Noboru Teramoto, Takayuki Ose, Hajime Fukuda, and Akihide Yamamoto for their cooperation during this project.

■ REFERENCES

(1) Tuan, R. S., Boland, G., and Tuli, R. (2003) Adult mesenchymal stem cells and cell-based tissue engineering. *Arthritis Res. Ther. 5*, 32−45.

(2) Jackson, L., Jones, D. R., Scotting, P., and Sottile, V. (2007) Adult mesenchymal stem cells: differentiation potential and therapeutic applications. *J. Postgrad. Med. 53*, 121−127.

(3) Shibata, T., Naruse, K., Kamiya, H., Kozakae, M., Kondo, M., Yasuda, Y., Nakamura, N., Ota, K., Tosaki, T., Matsuki, T., Nakashima, E., Hamada, Y., Oiso, Y., and Nakamura, J. (2008) Transplantation of bone marrow-derived mesenchymal stem cells improves diabetic polyneuropathy in rats. *Diabetes 57*, 3099−3107.

(4) Minguell, J. J., and Erices, A. (2006) Mesenchymal stem cells and the treatment of cardiac disease. *Exp. Biol. Med. (Maywood) 231*, 39−49.

(5) Delcroix, G. J., Schiller, P. C., Benoit, J. P., and Montero-Menei, C. N. (2010) Adult cell therapy for brain neuronal damages and the role of tissue engineering. *Biomaterials 31*, 2105−2120.

(6) Lipinski, M. J., Biondi-Zoccai, G. G., Abbate, A., Khianey, R., Sheiban, I., Bartunek, J., Vanderheyden, M., Kim, H. S., Kang, H. J., Strauer, B. E., and Vetrovec, G. W. (2007) Impact of intracoronary cell therapy on left ventricular function in the setting of acute myocardial infarction: a collaborative systematic review and meta-analysis of controlled clinical trials. *J. Am. Coll. Cardiol. 50*, 1761−1767.

(7) Ziegelhoeffer, T., Fernandez, B., Kostin, S., Heil, M., Voswinckel, R., Helisch, A., and Schaper, W. (2004) Bone marrow-derived cells do not incorporate into the adult growing vasculature. *Circ. Res. 94*, 230−238.

(8) Ishikane, S., Ohnishi, S., Yamahara, K., Sada, M., Harada, K., Mishima, K., Iwasaki, K., Fujiwara, M., Kitamura, S., Nagaya, N., and Ikeda, T. (2008) Allogeneic injection of fetal membrane-derived mesenchymal stem cells induces therapeutic angiogenesis in a rat model of hind limb ischemia. *Stem Cells 26*, 2625−2633.

(9) Bernsen, M. R., Moelker, A. D., Wielopolski, P. A., van Tiel, S. T., and Krestin, G. P. (2010) Labelling of mammalian cells for visualisation by MRI. *Eur. Radiol. 20*, 255−274.

(10) Bulte, J. W., Duncan, I. D., and Frank, J. A. (2002) In vivo magnetic resonance tracking of magnetically labeled cells after transplantation. *J. Cereb. Blood Flow Metab. 22*, 899−907.

(11) Stuckey, D. J., Carr, C. A., Martin-Rendon, E., Tylera, D. J., Willmott, C., Cassidy, P. J., Hale, S. J. M., Schneider, J. E., Tatton, L., Harding, S. E., Radda, G. K., Watt, S., and Clarke, K. (2006) Iron particles for noninvasive monitoring of bone marrow stromal cell engraftment into, and isolation of viable engrafted donor cells from, the heart. *Stem Cells 24*, 1968−1975.

(12) Bos, C., Delmas, Y., Desmouliere, A., Solanilla, A., Hauger, O., Grosset, C., Dubus, I., Ivanovic, Z., Rosenbaum, J., Charbord, P., Combe, C., Bulte, J. W., Moonen, C. T., Ripoche, J., and Grenier, N. (2004) In vivo MR imaging of intravascularly injected magnetically labeled mesenchymal stem cells in rat kidney and liver. *Radiology 233*, 781−789.

(13) Ju, S., Teng, G. J., Lu, H., Zhang, Y., Zhang, A., Chen, F., and Ni, Y. (2007) In vivo MR tracking of mesenchymal stem cells in rat liver after intrasplenic transplantation. *Radiology 245*, 206−215.

(14) Heymer, A., Haddad, D., Weber, M., Gbureck, U., Jakob, P. M., Eulert, J., and Noth, U. (2008) Iron oxide labelling of human mesenchymal stem cells in collagen hydrogels for articular cartilage repair. *Biomaterials 29*, 1473−1483.

(15) Arbab, A. S., Yocum, G. T., Rad, A. M., Khakoo, A. Y., Fellowes, V., Read, E. J., and Frank, J. A. (2005) Labeling of cells with ferumoxides-protamine sulfate complexes does not inhibit function or differentiation capacity of hematopoietic or mesenchymal stem cells. *NMR Biomed. 18*, 553−559.

(16) Farrell, E., Wielopolski, P., Pavljasevic, P., van Tiel, S., Jahr, H., Verhaar, J., Weinans, H., Krestin, G., O'Brien, F. J., van Osch, G., and Bernsen, M. (2008) Effects of iron oxide incorporation for long term cell tracking on MSC differentiation in vitro and in vivo. *Biochem. Biophys. Res. Commun. 369*, 1076−1081.

(17) Li, Z., Suzuki, Y., Huang, M., Cao, F., Xie, X., Connolly, A. J., Yang, P. C., and Wu, J. C. (2008) Comparison of reporter gene and iron particle labeling for tracking fate of human embryonic stem cells and differentiated endothelial cells in living subjects. *Stem Cells 26*, 864−873.

(18) Amsalem, Y., Mardor, Y., Feinberg, M. S., Landa, N., Miller, L., Daniels, D., Ocherashvilli, A., Holbova, R., Yosef, O., Barbash, I. M., and Leor, J. (2007) Iron-oxide labeling and outcome of transplanted mesenchymal stem cells in the infarcted myocardium. *Circulation 116*, I38−45.

(19) Terrovitis, J., Stuber, M., Youssef, A., Preece, S., Leppo, M., Kizana, E., Schar, M., Gerstenblith, G., Weiss, R. G., Marban, E., and Abraham, M. R. (2008) Magnetic resonance imaging overestimates ferumoxide-labeled stem cell survival after transplantation in the heart. *Circulation 117*, 1555−1562.

(20) Higuchi, T., Anton, M., Dumler, K., Seidl, S., Pelisek, J., Saraste, A., Welling, A., Hofmann, F., Oostendorp, R. A., Gansbacher, B., Nekolla, S. G., Bengel, F. M., Botnar, R. M., and Schwaiger, M. (2009) Combined reporter gene PET and iron oxide MRI for monitoring survival and localization of transplanted cells in the rat heart. *J. Nucl. Med. 50*, 1088−1094.

(21) Tachibana, Y., Enmi, J., Mahara, A., Iida, H., and Yamaoka, T. (2010) Design and characterization of a polymeric MRI contrast agent based on PVA for in vivo living-cell tracking. *Contrast Media Mol. Imaging 5*, 309−317.

(22) Yamaoka, T., Tabata, Y., and Ikada, Y. (1995) Comparison of body distribution of poly(vinyl alcohol) with other water-soluble polymers after intravenous administration. *J. Pharm. Pharmacol. 47*, 479−486.

(23) Agudelo, C. A., Tachibana, Y., Noboru, T., Iida, H., and Yamaoka, T. (2011) Long-term in vivo magnetic resonance imaging tracking of endothelial progenitor cells transplanted in rat ischemic limbs and their angiogenic potential. *Tissue Eng. Part A 17*, 2079−2089.

(24) Agudelo, C. A., Tachibana, Y., Hurtado, A. F., Ose, T., Iida, H., and Yamaoka, T. (2012) The use of magnetic resonance cell tracking to monitor endothelial progenitor cells in a rat hindlimb ischemic model. *Biomaterials 33*, 2439−2448.

(25) Oswald, J., Boxberger, S., Jorgensen, B., Feldmann, S., Ehninger, G., Bornhauser, M., and Werner, C. (2004) Mesenchymal stem cells can be differentiated into endothelial cells in vitro. *Stem Cells 22*, 377−384.

(26) Wingate, K., Bonani, W., Tan, Y., Bryant, S. J., and Tan, W. (2012) Compressive elasticity of three-dimensional nanofiber matrix directs mesenchymal stem cell differentiation to vascular cells with endothelial or smooth muscle cell markers. *Acta Biomater. 8*, 1440−1449.

(27) Dai, W., Hale, S. L., Martin, B. J., Kuang, J. Q., Dow, J. S., Wold, L. E., and Kloner, R. A. (2005) Allogeneic mesenchymal stem cell transplantation in postinfarcted rat myocardium: short- and long-term effects. *Circulation 112*, 214−223.

(28) Walczak, P., Kedziorek, D. A., Gilad, A. A., Lin, S., and Bulte, J. W. (2005) Instant MR labeling of stem cells using magneto-electroporation. *Magn. Reson. Med. 4*, 769−774.

(29) Pillai, O., and Panchagnula, R. (2001) Polymers in drug delivery. *Curr. Opin. Chem. Biol. 5*, 447−451.
(30) Yoshikawa, K., and Davies, A. (1997) Safety of ProHance in special populations. *Eur. Radiol. 7* (Suppl 5), 246−250.
(31) Modo, M., Beech, J. S., Meade, T. J., Williams, S. C., and Price, J. (2009) A chronic 1 year assessment of MRI contrast agent-labelled neural stem cell transplants in stroke. *Neuroimage 47* (Suppl 2), T133−142.
(32) Brekke, C., Morgan, S. C., Lowe, A. S., Meade, T. J., Price, J., Williams, S. C., and Modo, M. (2007) The in vitro effects of a bimodal contrast agent on cellular functions and relaxometry. *NMR Biomed. 20*, 77−89.
(33) Magerstadt, M., Gansow, O. A., Brechbiel, M. W., Colcher, D., Baltzer, L., Knop, R. H., Girton, M. E., and Naegele, M. (1986) Gd(DOTA): an alternative to Gd(DTPA) as a T1, 2 relaxation agent for NMR imaging or spectroscopy. *Magn. Reson. Med. 3*, 808−812.
(34) Endres, P. J., MacRenaris, K. W., Vogt, S., and Meade, T. J. (2008) Cell-permeable MR contrast agents with increased intracellular retention. *Bioconjugate Chem. 19*, 2049−2059.
(35) Amado, L. C., Saliaris, A. P., Schuleri, K. H., St John, M., Xie, J. S., Cattaneo, S., Durand, D. J., Fitton, T., Kuang, J. Q., Stewart, G., Lehrke, S., Baumgartner, W. W., Martin, B. J., Heldman, A. W., and Hare, J. M. (2005) Cardiac repair with intramyocardial injection of allogeneic mesenchymal stem cells after myocardial infarction. *Proc. Natl. Acad. Sci. U. S. A. 102*, 11474−11479.